Journal of Materials and Engineering Structures

Research Paper

Elaboration of geopolymer cement based on dredged sediment

Fouzia Mostefa [a], ***Nasr-Eddine Bouhamou*** [a,*], ***Salima Aggoune*** [b], ***Habib Mesbah*** [c]

[a] *Laboratory of Construction transport and Protection of Environment "LCTPE", Mostaganem University, Algeria*

[b] *Laboratory LGCGM, IUT of Rennes, France*

[c] *Laboratory of mecanic and materials of civil engineering L2GCGM, Cergy Pontoise university, Paris, France*

ARTICLE INFO

Article history :

Received : 24 May 2018

Revised : 13 October 2018

Accepted : 25 October 2018

Keywords:

Sediment

Geopolymer Cement

Paste

Mortar

ABSTRACT

This work aims to study the feasibility of making a geopolymer cement based on dredged sediments, from the Fergoug dam (Algeria). Sedimentary clays were characterized before and after calcination by X-ray diffraction, thermogravimetric analysis (ATG / ATD), spectroscopy (FTIR) and XRF analysis. The reactivity of the calcined products was measured using isothermal calorimetric analysis (DSC) on pastes prepared by mixing an alkaline solution of sodium hydroxide (NaOH) 8 M in an amount allowing to have a Na / Al ratio close to 1. Also, cubic mortar samples were prepared with a ratio of liquid to binder not: 0.8. The results obtained allowed to optimize the calcination time of 5 hours for a better reactivity of these sediments, and a concentration of 8 M of sodium hydroxide and more suitable to have the best compressive strength. Our study offer great prospects for upgrading the sediments used as geopolymer cements in mortars

1 Introduction

Many studies have shown that a large number of natural aluminosilicate materials can potentially be used for the synthesis of geopolymers such as kaolinite, stilbite, sodalite, illite, and anorthite [1]. Others of artificial nature have also been used: such as fly ash, volcanic slag, blast furnace slag, natural pozzolana and rice husk ashes [2].

The use of clays, such as kaolinite, depends on the reactivity which is a direct consequence of its mineralogical composition and its calcination temperature. The degree of the thermic treatment proportionally influences on the reactivity. The researchers experimented with different calcination temperatures. Davidovits et al calcined the clay at 500,650,700 and 750 ° C [3], Palomo et al [4] explored a temperature range of 600-700 ° C, Zhang and Sun- Wei [5] at 700 ° C, whereas Zibouche et al [6] preferred to treat it at 800 ° C with 3 calcination durations of 2, 4 and 6 hours respectively. The authors

* *Corresponding author. Tel.: +213 556248172.*
E-mail address: nasredine.bouhamou@univ-mosta.dz

e-ISSN: 2170-127X,

RESEARCH REVIEW of Sciences and Technologies

Chareerat et al [7] chose a range of 400,500,600,700 and 800 ° C with the same durations and concluded that the best calcination temperature is 600 ° C.

The sediments resulting from dredging by their more or less clayed composition may be an interesting alternative for the synthesis of geopolymers. The results of the XRD and FTIR spectral analysis of the preliminary study conducted by Chen et al [8] on samples calcined for 6 h, at varying temperatures between 500 and 900°C, showed that the crystalline structure collapsed at 850 ° C giving a better reactivity. For one or the other the results are different as regards the mechanical properties and microstructure. According to Davidovits [9] some clays react during the geopolymerization whereas others do not justify it by the insufficiency of the quantity of the kaolin content found in the raw material.

The main objective of this work is to study the possibility of using dredged sediments in the preparation of geopolymer cements. The approach consists first of all in optimizing a calcination time to have a better reactivity of the materials, a temperature of 750°C was chosen according to the bibliography, secondly to determine the effect of the different molarities of the activated solution on the compressive strength of a geopolymer mortars. The results are characterized by analysis tools (FTIR, RXD, TG and DSC)

2 Experimental setup

2.1 Used materials.

The sediment materials used is from Fergoug dam's in west of Algeria. On laboratory scale, a sample was dried first, grinded to a maximum particle size and sieving less than sieve of 80 um, subsequently calcined in a muffle electric furnace at 750 C° for 3, 4 and 5 hours (heating rate: 25 C/min). Finally, calcined samples were kept in plastic containers to protect them from moisture.

The raw sediment and calcined were subjected to FTIR-spectroscopy, thermal analysis (TG/ATD), X-Ray (XRD) analyses and laser granulometry. In addition, the raw material was submitted to elementary analyses: chemical analysis (table 2) and physical properties (table 3). The hydroxide sodium was used as alkaline solutions, it was obtained by dissolving dried pellets of 98% purity in distilled water to get solutions at 8, 10 and 12 M concentrations.

2.1.1 Geopolymer synthesis

In the first stage, and to measure the reactivity, the calcined sediments were subjected to polycondensation. The paste samples were prepared with NaOH solution 8M in quantity allowing to have a ratio Na/Al close to 1(1:1). The ratio is the recommended condition used for MK-based geopolymers, assuming that all of the precursor material is potentially reactive. The reactivity was tested using a differential scanning calorimetry (DSC) analysis.

In the second stage, the experimental polymerization procedure was performed. Geopolymer specimens were synthesized by adding the activing hydroxide solution (8 M) to calcined sediment: SC3 (750/3 h), SC4 (750/4h) and SC5 (750/5h) at a liquid-binder masse ratio of 0,8; for this ratio sediment exhibited favorable workability; without adding water. Other samples were prepared in the same way by adding hydroxide solutions 8, 10 and 12 M to SC5 material. The mortar with standardized sand was prepared following the instructions given in the EN Standards 196 -.1, and cast into a cubic (PVC) molds of the size (4x4x4) cm^3. All the specimens were sealed in plastics containers to prevent fast evaporation of water during curing and heated at 60 C° in laboratory oven for 24 hours, after they were demolded and aging at room temperature. Compressive strength tests were done at 1, 7 and 28 days.

2.1.2 Technical characterization.

Mineralogical and chemical characterization of raw materials was performed using X-ray fluorescence (XRF) and X-ray diffraction (XRD), a powder data sets were obtained with a PANalytical X'Pert Pro MPD with X'celerator diffractometer (Cu Ka radiation, 45 kV, 40 mA). The analytical range used was between 5° and 75° with a step size of 0,0080°. X'Pert High Score Plus software and *Inorganic Crystal Structure Database* (ICSD) were used for mineral identification and semi quantitative evaluation. Thermogravimetric and Differential Analysis were obtained with Perkin Elmer Pyris Diamond. The entire test and the grain size analysis was carried at out laboratory INSA Rennes.

Table 1: [a] and [b] Molar ratios of mortar samples

	Mortar	% Oxides				
		Na/Si	Na/Al	%Na2O	L/B	NaOH
[a]	SC3	0,233	1,028	10,076	0,8	8
	SC4	0,234	1,020	10,076	0,8	8
	SC5	0,225	0,987	10,076	0,8	8
	Mortar SC5	% Oxides				
		Na/Si	Na/Al	%Na2O	L/B	
[b]	8M	0,225	0,987	10,076	0,8	
	10M	0,271	1,185	12,212	0,8	
	12M	0,311	1,361	14,116	0,8	

RS: raw sediment; SC3; SC4; SC5 sediment calcined at 3 ; 4 and 5 hours for 750°C

The Fourier transform infrared spectroscopy (FTIR) was used to investigate the structural evolution of the raw, calcined sediment, tests were recorded in the range (were taken in the mid region) of 400–4000 cm1 using a Bruker Optic. For the paste, a isothermal test was carried out according to the following criteria, the components were mixed for 3 min prior to test, 40 to 45 mg were heated up At 60 °C to 2 °C/min after which, the temperature was maintained at a constant value of 60°C**.** The reactivity was evaluated by measuring the heat evolved in each paste samples.

TG and DSC analysis on mortar specimens were carried out from 20°C up to 1000°C under nitrogen atmosphere, with a constant heat rate (10 C/min) the study were conducted on 15-30 mg of powder. Simultaneous DSC–TG measures both the heat flows associated with phase transitions in the different geopolymer binder as a function of temperature and time. The mechanical strengths of the mortars have been determined at the age of 1, 7 and 28 days.

3 Experimental Results and discussions.

The quantitative chemical and mineralogical composition of the raw sediment is reported in Table 2. The semi-quantitative mineralogical estimation is based on bulk chemical analysis of raw material in combination with the characteristic XRD peaks of each mineral. The results revealed that clay phases represent the main crystalline component: kaolinite (20,27 %), illite (19,92%), the quartz (24,42 %), in the other hand the percentage of calcite (23,5 %) was determined by the Bernard calcimetry test. The presence of silica and alumina in sediments makes it possible to use them as a geopolymer precursor.

Table 2: Chemical composition of *raw* sediments

Oxide	SiO_2	Al_2O_3	CaO	Fe_2O_3	Na_2O	K_2O	MgO	TiO_2	LIO
%	42,65	15,50	13,37	6,39	0,53	2,30	2,85	0,77	14,3

The responses of the physical characterization tests of the sediments used are presented in (Table 3) and (Fig. 1). The results obtained show that sediments are considered as fine soils composed mainly of clay, silt and fine sand, and can be classified according to the Casagrande abacus as very plastic clay soil

Table 3 : Physicals properties of raw *sediments*

W_L[%]	W_p[%]	I_p
84,13	37,33	46,82

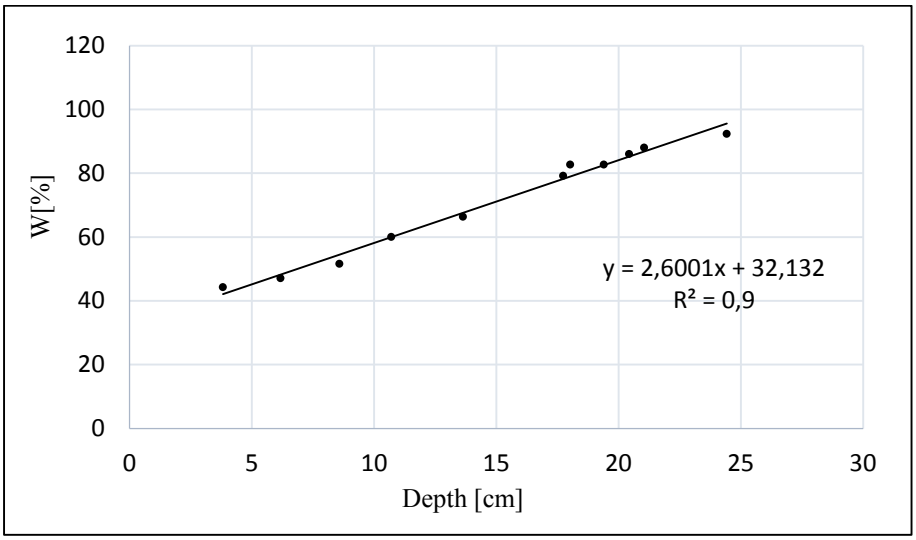

Fig. 1-Liquidity limit of raw sediment

Table 4: Particle Size Analysis of sediments

Sample	D90	D50	D10	Density [g/cm^3]	Area surface [cm^2/g]
RS	4,8	2,5	1,3	2,56	9.780
SC3	8,1	4,1	2,0	2,53	8.160
SC4	8,2	4,3	2,1	2,48	8.039
SC5	9,4	5,0	2,3	2,46	7.315

Based on calculations of the average diameters of the materials using the method of the central tendency (Table 4) and grain size distribution (Fig. 2), the results show that the raw sediments have a bimodal distribution, and are composed of at least two populations. First one is centered between 10 µm representing a larger clay fraction (clays and silt), the second one is centered at 80 µm representing the non-clay fraction generally quartz. Nevertheless, it has been noticed that an important modification is induced by the thermal treatment, linked to the size of the particles, it seems that the average diameters increase in value gradually with the calcination temperature which is probably due to a densification of the microstructure of the microspheres by phenomena associated with the disappearance of the mesoporosity (intra-aggregates porosity), thus confirming the different hypotheses emitted, that a heat treatment tends to agglomerate the particles (Fig. 3).

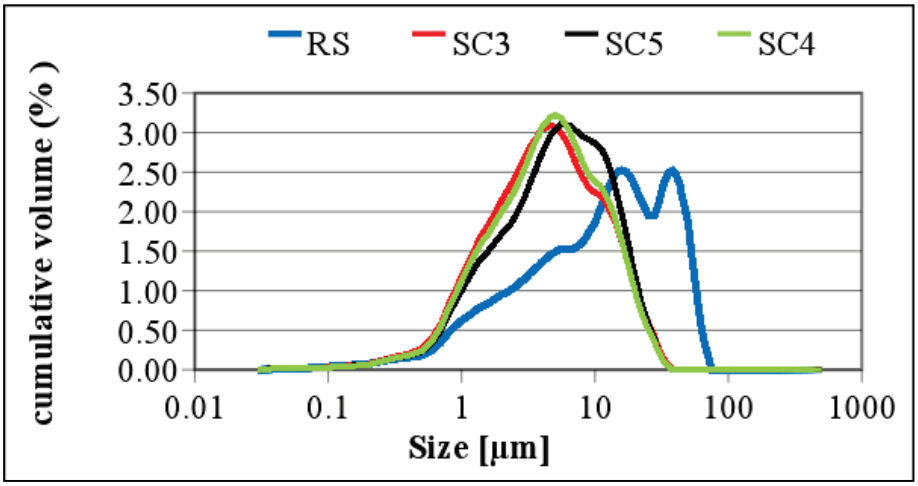

Fig. 2 – Particle size distribution

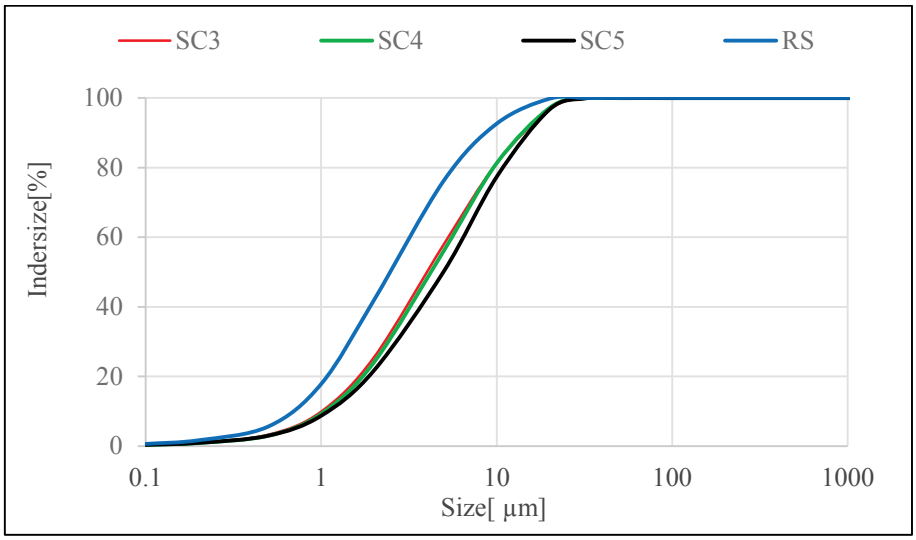

Fig. 3– Accumulative grain size distribution of raw and calcined sediment

In addition the granular distribution seems to be transformed into a unimodal distribution centered 5 µm.The specific surface area decreases considerably due to the consolidation and thermal sintering of the mineral phase, whereas the density seems to decrease slightly probably due to the dehydroxylation of the clay phase, which can generate porosity on the sediment particles.

3.1 Thermogravimetric and Differential Analysis (TG/ATD) analysis.

The gravimetric analysis of the raw sediments illustrated in Figure 4 shows the appearance of three main endothermic peaks, the first one, corresponds to the adsorbed water loss detected between 50°C and 120 °C with a loss of mass of 4.2 % which is related to the removal of hygroscopic water from illite. The second one is detected at 495°C and corresponds to the loss of the structural hydroxyl groups, causing the transformation of kaolinite into metakaolinite, with a loss of mass of 3.20%. The last one is in the range of 680-750 °C, it refers to the decarbonation of calcite to calcium oxide with a loss of mass of 9.79%.

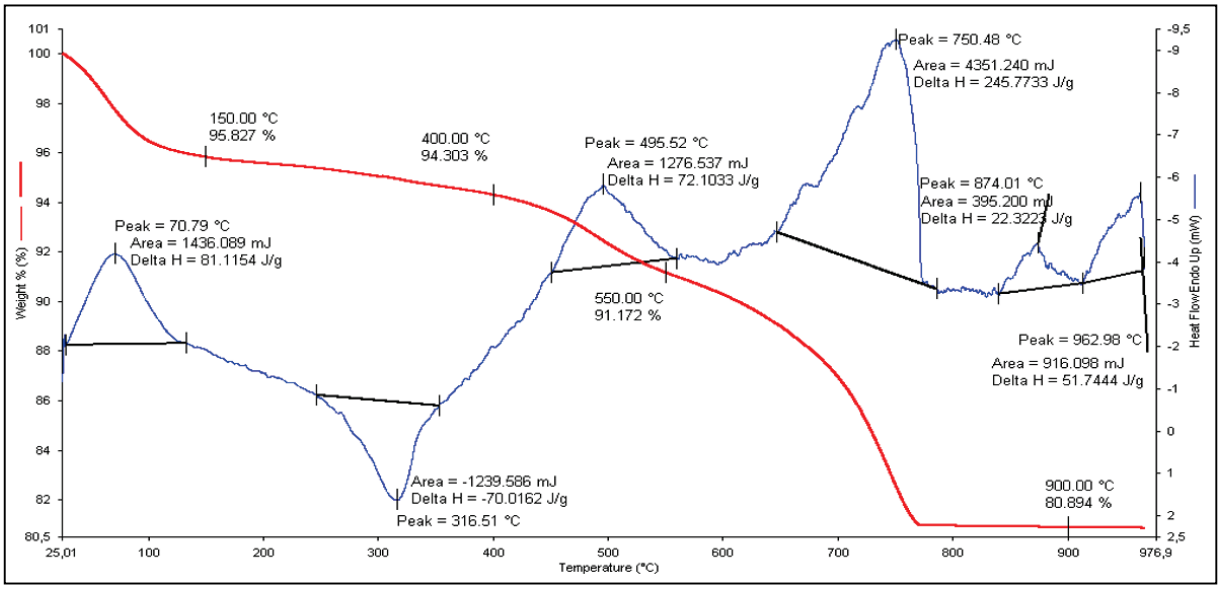

Fig. 4 - TGA, DTG curves of raw sediment

At the same time, two exothermic peaks were recorded, the first labelled at 320 °C corresponding to the combustion phase of the organic matter contained in the sample. A last exothermic event is observed from 960ºC without loss of mass.

This thermal event may be related to the transformation of metakaolinite into a more stable structure such as primary mullite. As for the illitic structure, it seems to persist after calcination at 750 °C. The process of dehydroxylation of illite continues up to 870 °C where it is observed a less marked endothermic peak with a very slight loss of mass corresponding to an incomplete dehydroxylation of its structure. These results are in agreement with those obtained by the XRD and FTIR analyses of calcined sediments.

3.2 X-ray (XRD) analysis

X-ray diffraction analysis (Fig. 5) shows that dredged sediments (RS) consist mainly of minerals associated with kaolinite (d =7, 15 A °, 2thta = 12.38 °), illite (d =10,12 A °, 2theta = 8.74 °) and calcite (d=3,04 A°, and 2theta= 29,41°).The intensity of this diffractogram shows that quartz is the most dominant phase, which peaks are observed at 20.86 (4.26 A °).

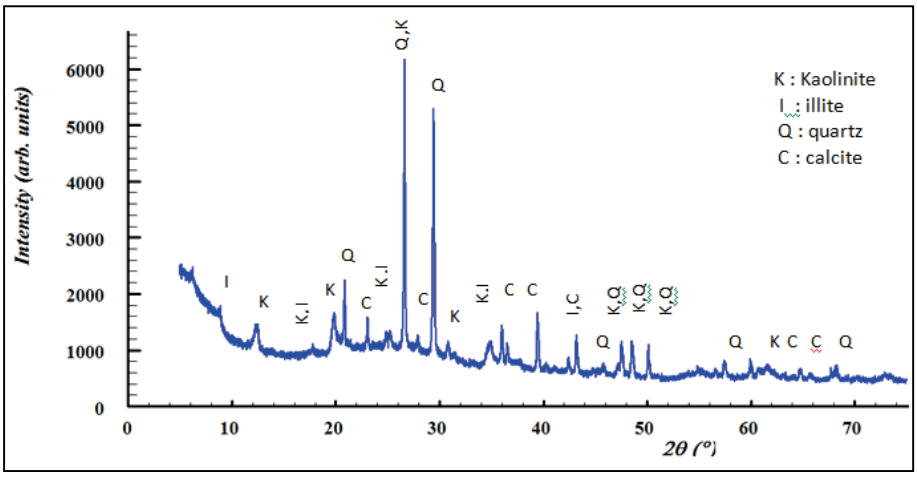

Fig. 5 - XRD pattern of raw sediment

In contrast, the XRD diagram of calcined sediment presented in Fig. 6 shows that the diffraction peaks corresponding to kaolinite and calcite have undergone progressive amorphization, manifested by the disappearance of their characteristic peaks beyond a calcination temperature of 750°C for 3h. The destruction of the crystalline phases by calcination leads to the formation of amorphous substances causing an increase of the background noise in the XRD spectrum. The recorded spectra indicate that the dehydroxylation did not lead to thecomplete collapse of the illite. The persistence of a peak around 10Å on all diffractograms confirms its presence [10, 11]. In general, illite is dehydroxylated at higher temperatures than kaolin. In the 3 to 5 hour calcination interval, the remaining peaks were attributed to quartz.

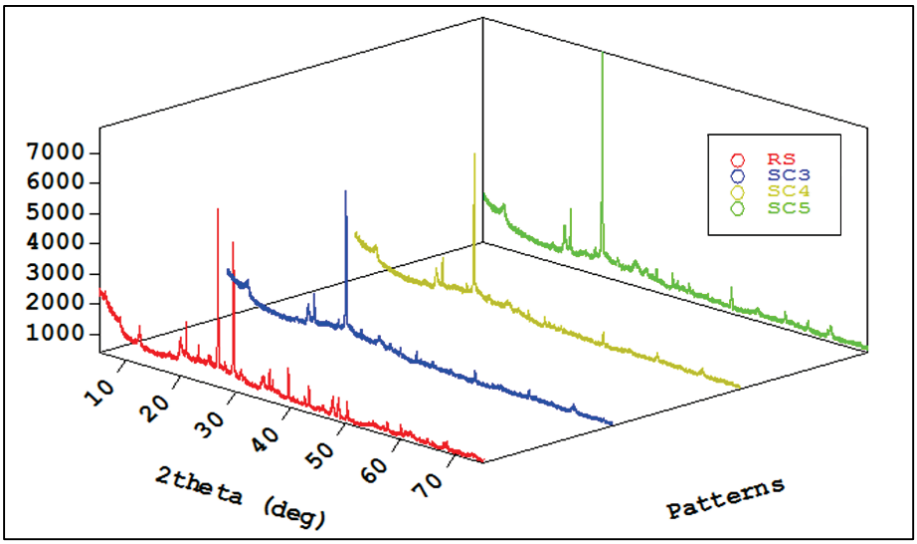

Fig. 6 - XRD of raw and calcined sediment

3.3 Fourier Infra-Red Spectroscopy Analysis

The presence of quartz in the raw sediment (Fig. 7), is shown by symmetrical Si-O bending vibrations around 693 cm^{-1}, symmetrical Si-O stretching vibrations around 779 and 798 cm^{-1} and asymmetric stretching vibrations Si -O around 997 and 1163 cm^{-1} [12]. The adsorption peaks at approximately 3419 cm^{-1} and 1633 cm^{-1} reflect the stretching and bending vibration frequencies of the hydroxyl groups, respectively [13] the presence of these bands associated at 779 cm^{-1}indicate the possibility of the presence of illite [14], the Illitique structure is also observed in FTIR spectra with a large band 832 cm^{-1} [15] attributed to the mode of deformation of the Mg-OH -Al group and 693 cm^{-1} band [16] Also from the FTIR graph, there appears a broad band centered around 1429 cm^{-1}associated with the peaks, 873 and 712 cm^{-1}; these bands are related to the stretching vibration of carbonate groups present in calcite [17], in addition to low peaks centered at 1796 and 2514 cm^{-1} also represent the same grouping.

The frequencies at 3621 cm^{-1} and 3696 cm^{-1} are due to OH stretching of the hydroxyl groups of the inner surface [18]. Their presence associated with the peak at 798 cm^{-1}, prove that sediments contain of kaolinite. This presence also materialized on the one hand by the bands around 1163cm^{-1} and 997 cm^{-1} which characterize the stretching vibrations of Si-O and Si-O-Si, respectively [13, 19, 20], and in other hand by the intense band located at 913 cm^{-1} reflects the presence of Al-OH deformation vibration [21]. According to Ramasamy et al [12], both peaks 3696 and 3620 cm^{-1} suggest that kaolinite may be in a disordered state.

After calcination and as shown in Fig. 8, the FTIR analysis confirms the collapse of the kaolinite structure, beyond 750°C/3h, by the total disappearance of the peaks at 3696, 3621 and 1163 cm^{-1}. due to dehydroxylation of the crystalline phases. For the peak 914 cm^{-1} it is visibly replaced by another stretching vibration at 798 cm^{-1} corresponding to Al^{IV}-O [9]. The 998cm^{-1} band appears to be transformed into a broad band of amorphous silica localized at 1007 for 750° C/5h cm^{-1} [22], and moving towards 994 and 996cm^{-1} for 750°C/3 and 4 h.

In other hand, the structure of the illite seems slightly damaged, which is confirmed by the persistence and decrease of the intensities of the 1633 cm^{-1} and 3419 cm^{-1} bands. The figure 8 also shows the disappearance of the calcite peaks at 1429 and 873 cm^{-1} [15].

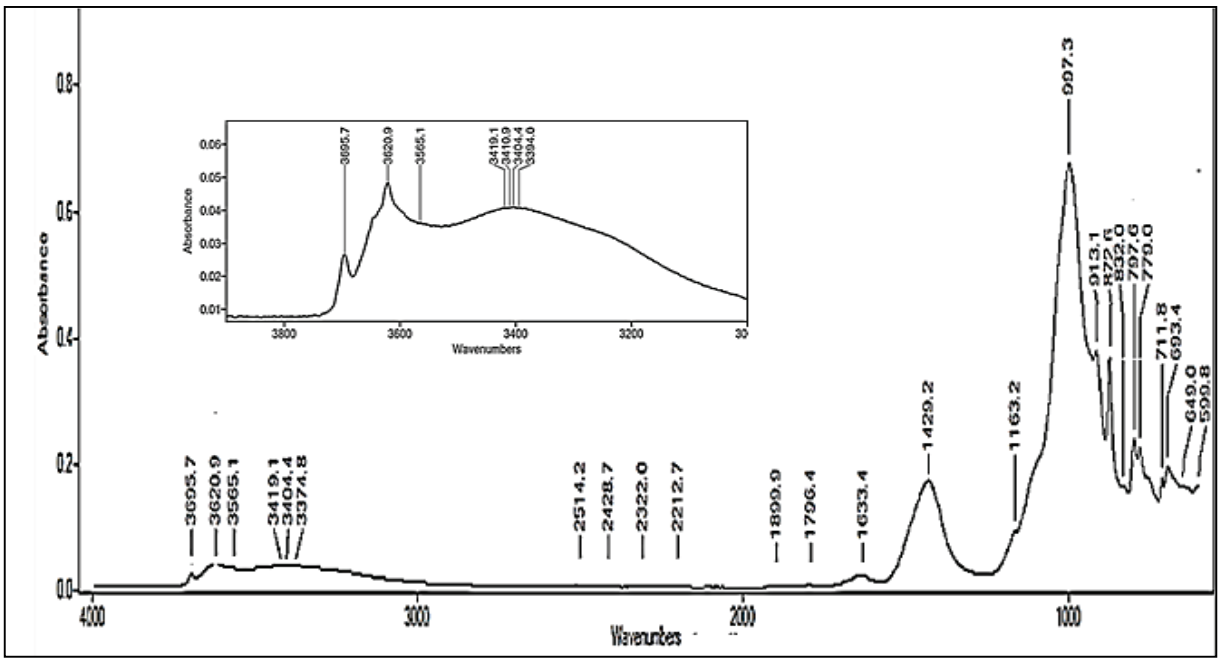

Fig 7 - FTIR analysis for the raw materials.

Finally, the analysis of the FTIR spectra shows that the effect of the heat treatment was immediately manifested by significant reductions in the intensities of the bands due to adsorbed H_2O.The FTIR result is in agreement with the XRD analysis which indicates a sequential degradation of clay after a treatment.

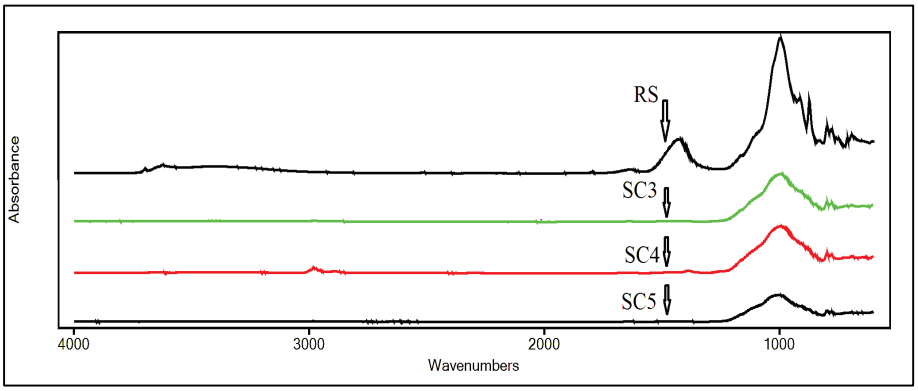

Fig. 8 - FTIR analysis for the raw and calcined materials

3.4 DSC (Differential Scanning Calorimetry)

For isothermal calorimetric analysis (Fig. 9), only the first two hours of test are represented, since beyond this period, the heat flow seems to stabilize and no loss of heat has really been recorded. It is clear that the curves of the three samples evolve in the same way. From the first minutes, it is observed the appearance of a first early exothermic peak during the rise in temperature, which corresponds to the absorption of the alkaline solution on the surface of the particles, this step corresponding to the first stage of dissolution. [22]. The OH- anions attack the Al-O and Si-O bonds on the surfaces of the particles, breaking them in the aqueous solution, thus allowing the formation of aluminosilicate units and their complexation with the alkaline ions [23, 24]. This step is followed by a large endothermic peak attributed to the continuity of the dissolution phase, suggesting a breakdown of Si-O-AL-O species [25**].**

The broad exothermic peak corresponds to the reaction-precipitation phase revealing a formation of aluminosilicate hydrates gel (NASH) [26]. After 50 minutes the heat flow seems to have remained stable, the paste (SC5) shows a narrow peak around °C (t: 100 min), it can be associated with the release of water [12] during the polymerization. The largest exothermic peak is obtained by the paste (SC5) with a flow of 0.063 followed by (SC4) and (SC3) with fluxes 0.056 and 0.0337mw/mg respectively.

The reactivity of the treated sediments can be quantified from the energy generated by the release of heat, it is measured from the area below the flux peaks, and for (SC4) and (SC5); the corresponding areas are almost identical with values of 25,64 and 30.77 J/g respectively, whereas for (SC3) the value is 19.69 J/g. According to these results, it can be said that the calcination time of 3, 4 and 5 h gradually influence sediment reactivity, which is in agreement with the results obtained from compressive strength tests that will be discussed latter.

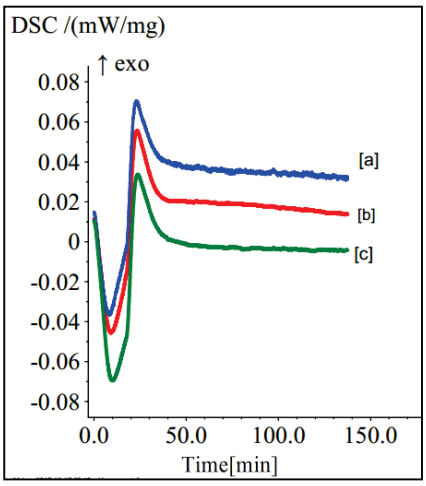

Fig 9 - DSC (Isothermal calorimetry) of geopolymer paste samples [a]: SC5, [b]: SC4,[c] : SC3

3.5 Thermogravimetric and DSC analysis of mortars.

The TG/DSC analyses were conducted for different concentrations of NaOH solution (8, 10 and 12) M, on geopolymer powders embedded in the mortar CS5 obtained by grinding and sieving less than 80 microns of the 7-day hardened mortars. The results of thermogravimetry (TG) are shown in Fig 10. The thermograph displays different distinguished regions, characterized by variables in levels and quantities of mass losses. In general, it can be seen that the three thermal curves evolve in the same way up to 1000°C. Significant losses of mass are observed and localized in the range 50 - 200 C °, more approximately between 70 and 120 C°; they correspond to the free water absorbed on the surface and that which is trapped in the large structural pores of the geopolymer gel [27, 28]. The associated mass losses are of the order of 5,32%; (SC5-M8), 6,12 % (SC5-M10) and 6,09% (SC5-M12),this shows that the SC5-M8 sample has a denser structure, and a better polycondensation compared to the other two samples [29].

In the second region located between 200 - 650 °C, there is a gradual decomposition of the structure of the gel formed during hardening (NASH) [30]. The losses of masses corresponding to water closely related to the structure, which are due generally to the dehydroxylation of the Si-OH and Al-OH groups [31]. They are of the order of 8,15 % (SC5-M8), 6.82% (SC5-M10) and 7.13% (SC5-M12), and suggest the possibility of a large degree of geopolymerization achieved by (SC5-M8), than to others samples [29]. On the other hand, those recorded between 650°C and 820 °C, are related to the decarbonation of the mineral phase of sodium carbonates (Na2CO3) formed during hardening [32], no significant loss of mass was observed above 820°C.

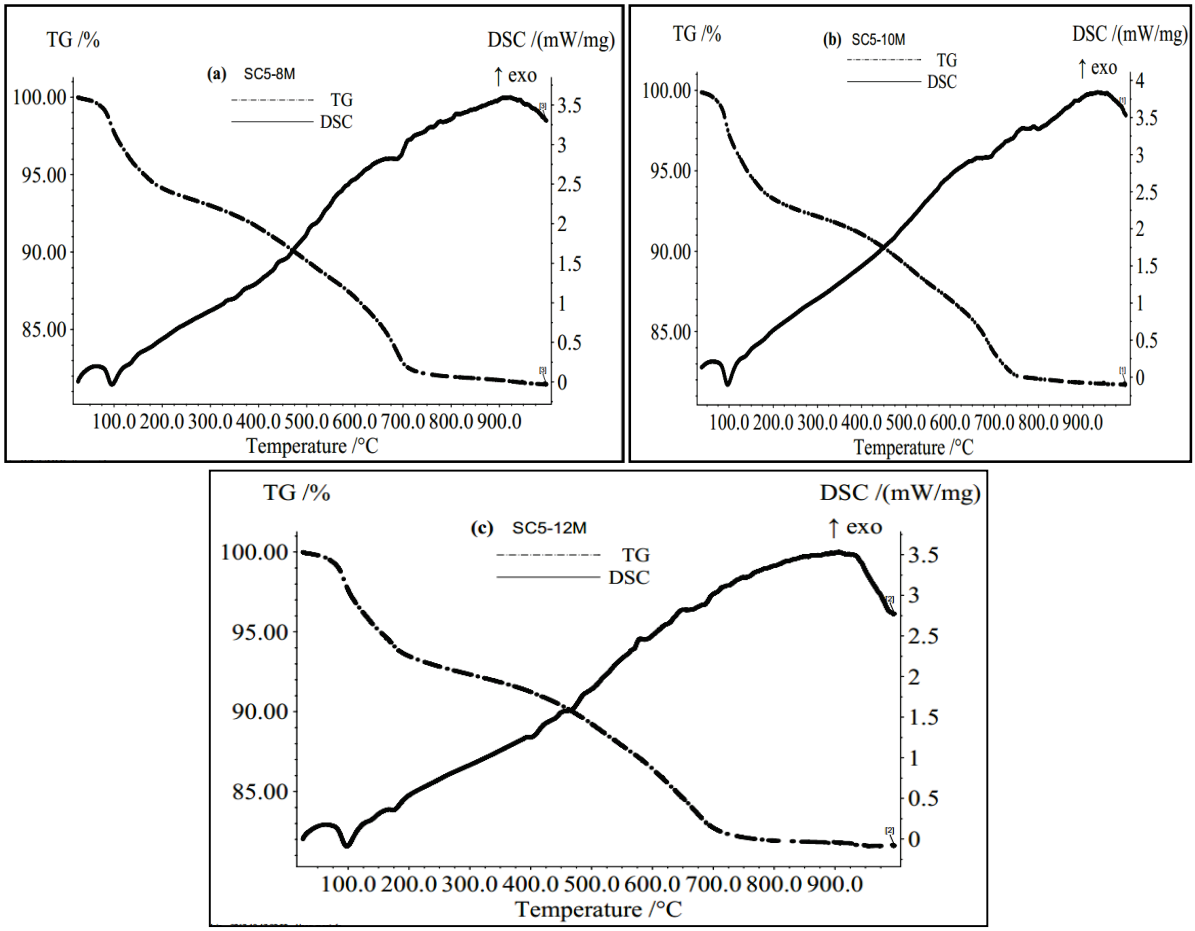

Fig.10- TG/DSC of geopolymer samples (a) SC5-8M, (b) SC5-10M and (c)SC5-12M

For the DSC level (Fig. 11) and the heat flux released, the samples show similar and slightly different curves. Two main peaks are observed. A first large and important endothermic peak located in the first region between 70 and 120 °C corresponding to the loss of free absorbed water. A second exothermic peak observed in the 820-950 C° region can be caused either by crystallization or rearrangement of the mineral phases [30, 33] or by formation of new phases [34].

Nevertheless, a small endothermic peak is observed between 650 and 750 °C suggesting the presence of some residues of calcined sediments, which have not yet reacted.

3.6 Compressive strength test

Figure 11 shows that mortar samples (SC5) exhibit the best Compressive strength at 7 and 28 days compared to mortar samples (SC3) and (SC4. It is known that the final composition of the geopolymers with respect to the ratios: Na2O/Al2O3 and Na2O/SiO2 affects the compressive strengths. From the calculations and for the same molarity, these ratios are almost identical .The difference results from their chemical compositions which differs little according to the calcination. Thus, it can be realized that the Compressive strength obtained for the mortars are due essentially to the reactivity of the calcined products, which is, more important for the SC5 sediment, so the calcination time of 5 hours is better indicated for the transformation of the crystalline phases to amorphous phases for this kind of sediment.

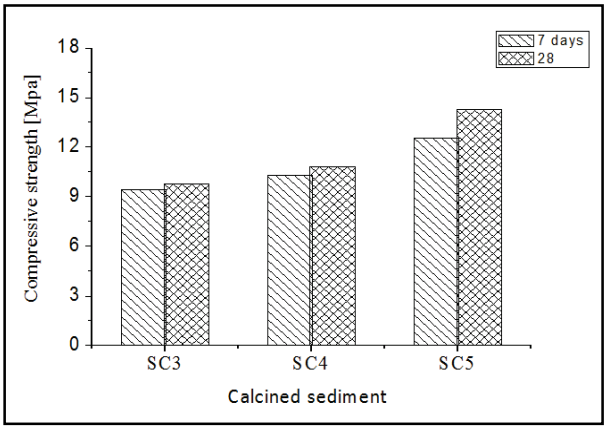

Fig.11- Effect of calcination time on compressive strength

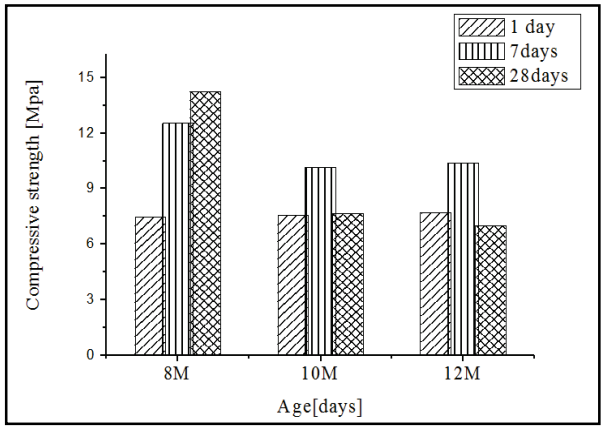

Fig.12-Effect of NaOH molarity on compressive strength for CS5

Figure 12 illustrates the result of the compressive strengths obtained for crushing the mortar samples (SC5) prepared with different molarity of NaOH solution. It is clear that the highest strength is obtained with solution in 8M concentration, after 7 and 28 days hardening compared to 10 M and 12 M**.** Nevertheless, after 24 hours of curing at 60 °C, the values of the three mortars are almost identical. It's probable that at this temperature, the system releases more heat, which results in a greater extent of geopolymerization [35]. Where as at 28 days the mechanical performances seem to decrease with the increase of the concentration. Granted to authors [36, 37] an increase of the activation solution beyond an optimum, delays the polymerization process because a large amount of dissolved ions in a highly alkaline solution causes saturation and limits the contact between the polymerized species and formation of coagulated structure. At age 7 days of cure, traces of efflorescence appeared, more visible for the sample with 10M and 12M than those with 8M (Fig, 13). These traces are caused by the formation of sodium carbonates formed by atmospheric carbonation, which may hinder the polymerization process [38]. This phenomenon generally causes the degradation of the binder and leads to falls in final resistances.

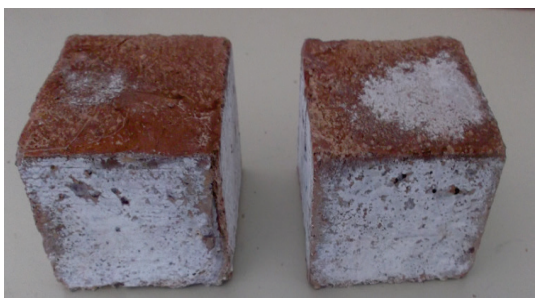

SC5-10M and SC5-12M after 7 days

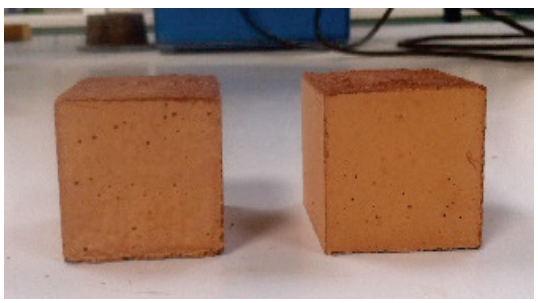

SC5-8M after 7 days

Fig.13 -Efflorescence geopolymer specimens; Rewrite

The content of Na2O (contained in the alkaline solution) is considered as a determining factor affecting the mechanical properties. According to Arham [39] the resistances are higher for high levels. For this study, it is the lowest Na2O content that has led to better performance. According to Barbosa [40] an optimal polymerization is obtained when the concentration of Na is sufficient to provide a balanced environment between the species forming the geopolymer gel, allowing the substitution of Al tetrahedral Si, and thus avoid the formation of carbonates.

4 Conclusion

This study confirmed the possibility to using dredged sediments as a precursor of geopolymer cement, the main conclusions obtained are:

- The DRX and FTIR analyzes have shown that a heat treatment effects a sequential degradation of the clay as a function of the calcination time, and a duration of 5 h seems the optimal time for a desydroxylation of the structure and the transformation advanced kaolinite to metakaolin, in contrast to the illite structure that partially collapsed. This finding was confirmed by the evaluation of the reactivity calcined samples, by measuring the extent of polycondensation as a function of the heat flux generated by samples of mortars, it was found that the samples formulated with SC5 and a solution of 8M presents a more important geopolymerization than the SC3 and SC4.
- The mechanical performance obtained for the mortars are due essentially to the reactivity of the calcined products, which is, more important for the SC5 sediment, so the calcination time of 5 hours is better indicated for the transformation of the crystalline phases to amorphous phases for this kind of sediment.
- It is possible to develop a geopolymer cement provided that the amount of activation solution is adjusted according to the amount of active aluminum silicate in the calcined materials, an optimum value of hydroxide concentration can accelerate the polymerization reaction and increases the mechanical properties, but an excess of concentration beyond the optimum value reduces the mechanical strengths.

The results obtained offer great prospects for upgrading the sediments used as geopolymer cements in mortars. It should continue in this way with other characterization tests on new concretes, especially self-compacting concretes.

REFERENCES

[1]- H. Xu, J.S.J. Van Deventer, The geopolymerisation of alumin-osilicate minerals. Int. J. Mineral Proc. 59 (2000) 247-266. doi:10.1016/S0301-7516(99)00074-5

[2]- J.G.S. Van Jaarsveld, J.S.J. Van Deventer, G.C. Lukey, The effect of composition and temperature on the properties of fly ash and kaolinite-based geopolymers. Chem. Eng. J. 89(1-3) (2002) 63-73. doi:10.1016/S1385-8947(02)00025-6

[3]- J. Davidovits, Geopolymer - Chemistry & Applications. 3rd Ed., Geopolymer Institute, 2011.

[4]- A. Palomo, F.P. Glasser, Chemically-bonded cementitious materials based on metakaolin. Brit. Ceram. T. 91 (1992)107-112.

[5]- Y. Zhang, W. Sun, Fly ash based geopolymer concrete. Indian Concr. J. (2006)1-5.

[6]- F. Zibouche, H. Kerdjoudj, J.-B. d'Espinose de Lacaillerie, H. Van Damme, Geopolymers from Algerian metakaolin: influence of secondary minerals. Appl. Clay Sci. 43(3-4) (2009) 453-458. doi:10.1016/j.clay.2008.11.001

[7]- T. Chareerat, A. Lee-Anansaksiri, P. Chindaprasirt, Synthesis of high calcium fly ash and calcined kaolin geopolymer mortar. In: Proceedings of the 1st International Conference on Pozzolan, Concrete and Geopolymer, Khon Kaen, Thailand, 2006, pp. 327-335.

[8]- J.H .Chen, J.S. Huang, Y.W .Chang, A preliminary study of reservoir sludge as a raw material of inorganic polymers. Constr. Build. Mater. 23(10) (2009) 3264-3269. doi:10.1016/j.conbuildmat.2009.05.006

[9]- G.W. Brindley, G. Brown, Crystal Structures of Clay Minerals and their X-ray Identification. Ed. Mineralogical Society Monograph, London, 1980. doi:10.1180/mono-5

[10]- D.M. Moore, R.C. Reynolds Jr., X-Ray diffraction and the identification and analysis of clay minerals. Ed. Oxford University Press, 2nd Ed. 1997.

[11]- V. Ramasamy, S. Murgesan, S. Mullainathan, Characterisation of minerals and relative distribution of quartz in

cauvery river sediments from tamilnadu, india–a ftir study. Bull. Pure Appl. Sci. 23F(1-2) (2004) 1-7.
[12]- R. Hamzaoui, F. Muslim, S. Guessasma, A. Bennabi, J. Guillin, Structural and thermal behavior of proclay kaolinite using high energy ball milling process. Powder Technol. 271(2015) 228- 237. doi:10.1016/j.powtec.2014.11.018
[13]- P.S. Nayak, B.K. Singh, Instrumental characterization of clay by XRF, XRD and FTIR. B. Mater. Sci. 30(3) (2007) 235–238. doi:10.1007/s12034-007-0042-5
[14]- H. Van Olphen, J.J. Fripiat, Data Handbook for Clay Materials and Other Non-Metallic Minerals. Pergamon Press, Oxford, 1979.
[15]- N.Y. Mostafa, Q. Mohsen, A. El-maghraby, Characterization of low-purity clays for geopolymer binder formulation. Int. J. Miner. Metall. Mater. 21(6) (2014) 609-619. doi:10.1007/s12613-014-0949-y
[16]- V.C. Farmer, Infrared spectroscopy, Characterization of the chemical structures of natural and synthetic aluminosilicate gels and sols by infrared spectroscopy. Geochim. Cosmochim. Acta 43(9) (1979) 141761420. doi.org/10.1016/0016-7037(79)90135-2
[17]- J.D. Russell, A.R. Fraser, Infrared methods. In: Wilson M.J. (Eds) Clay Mineralogy: Spectroscopic and Chemical Determinative Methods. Springer, Dordrecht, 1994. doi:10.1007/978-94-011-0727-3_2
[18]- P. Duxson, The structure and thermal evolution of metakaolin geopolymers. PhD thesis, Department of Chemical & Biomolecular Engineering, The University of Melbourne, 2006.
[19]- E. Balan, A. M. Saitta, F. Mauri, G. Calas, First-principles modeling of the infrared spectrum of kaolinite. Am. Mineral. 86(11-12) (2001) 1321-1330. doi:10.2138/am-2001-11-1201
[20]- J.D. Russell, V.C. Farmer, Infra-red spectroscopic study of the dehydration of montmorillonite and saponite. Clay Miner. Bull. 5(2) (1964) 443-464. doi:10.1180/claymin.1964.005.32.04
[21]- B. Tyagi, C.D. Chudasama, R.V. Jasra, Determination of structural modification in acid activated montmorillonite clay by FT-IR spectroscopy. Spectrochim. Acta-A. 64(2) (2006) 273-278. doi:10.1016/j.saa.2005.07.018
[22]- A. Buchwald, R. Tatarin, D. Stephan, Reaction progress of alkaline-activated metakaolin ground granulated blast furnace slag blends. J. Mater. Sci. 44(20) (2009) 5609-5617. doi:10.1007/s10853-009-3790-3
[23]- X. Yao, Z. Zhang, H. Zhu, Y. Chen, Geopolymerization process of alkali-metakaolinite characterized by isothermal calorimetry. Thermochim. Acta, 493(1-2) (2009) 49-54. doi:10.1016/j.tca.2009.04.002
[24]- D. Ravikumar, N. Neithalath, Reaction kinetics in sodium silicate powder and liquid activated slag binders evaluated using isothermal calorimetry. Thermochim. Acta 546 (2012) 32-43. doi:10.1016/j.tca.2012.07.010
[25]- E.A.S. Vassalo, A.G. Gumieri, M.T.P. Aguilar, Characterization of geopolymers obtained by alkaline activation of metakaolin with high iron content. In: Sustainable Solution in Structure Engineering and Construction, Ed. K. Chantawarangul, W. Swanpaga, S. Yazdani, V. Vimonsatit and A. Singh, ISEC Press, 2014.
[26]- P. Duxson, A. Fernández-Jiménez, J.L. Provis, G.C. Lukey, A. Palomo, J.S.J. Van Deventer, Geopolymer technology: the current state of the art. J. Mater. Sci. 42(9) (2007)2917-2933. doi:10.1007/s10853-006-0637-z
[27]- J. Rocha, J. Klinowski, Solid-state NMR studies of the structure and reactivity of metakaolinite, Angew. Chem. Int. Edit. 29(5) (1990) 553-554. doi:10.1002/anie.199005531
[28]- N. Saidi, B. Samet, S. Baklouti, Effect of composition on structure and mechanical properties of metakaolin based PSS-Geopolymer. Int. J. Mater. Sci. 3(4) (2013) 145-151. doi:10.14355/ijmsci.2013.0304.03
[29]- R.L. Frost, M.C. Hales, W.N. Martens, Thermogravimetric analysis of selected group (II) carbonate minerals implication for the geosequestration of greenhouse gases. J. Therm. Anal. Calorim. 95 (2009) 999-1005. doi:10.1007/s10973-008-9196-7
[30]- R. Onori, J. Will, A. Hoppe, A. Polettini, R. Pomi, A.R. Boccaccini, Bottom ash-based geopolymer materials: mechanical and environment properties. In: Ceramic Engineering and Science Proceedings - Developments in Strategic Materials and Computational Design II: Ceramic Engineering and Science Proceedings, Vol. 32, 2011, pp. 71-80. doi:10.1002/9781118095393.ch7
[31]- M.A. Villaquiran-Caicedo, R.M. de Gutiérrez, S. Sulekar, C. Davis, J.C. Nino, Thermal properties of novel binary geopolymers based on metakaolin and alternative silica sources. Appl. Clay Sci. 118 (2015) 276-282. doi:10.1016/j.clay.2015.10.005
[32]- A. Adriano, G. Soriano, J. Duque, Characterization of water absorption and desorption properties of natural zeolites in Ecuador. In: Proceedings of the Fifth International Symposium on Energy, Puerto Rico Energy Center-Laccei, Puerto Rico, 2013, pp. 1-9.
[33]- M. Zhang, M. Zhao, G. Zhang, T. El-Korchi, M. Tao, A multiscale investigation of

reaction kinetics, phase formation, and mechanical properties of metakaolin geopolymers. Cem. Concrete Compos. 78 (2017) 21-32. doi:10.1016/j.cemconcomp.2016.12.010

[34]- H.Y. Zhang, V. Kodur, B. Wu, L. Cao, F. Wang, Thermal behavior and mechanical properties of geopolymer mortar after exposure to elevated temperatures. Constr. Build. Mater. 109 (2016) 17-24. doi:10.1016/j.conbuildmat.2016.01.043

[35]- M.H. Cornejo, J. Elsen, C. Paredes, H. Baykara, Thermomechanical treatment of two Ecuadorian zeolite-rich tuffs and their potential usage as supplementary cementitious material. J. Therm. Anal. Calorim. 115(1) (2014) 309-321. doi:10.1007/s10973-013-3345-3

[36]- M.S. Muñiz-Villarreal, A. Manzano-Ramírez, S. Sampieri-Bulbarela, J.R. Gasca-Tirado, J.L. Reyes-Araiza, J.C. Rubio-Ávalos, J.J. Pérez-Bueno, L.M. Apatiga, A. Zaldivar-Cadena, V. Amigó-Borrás, The effect of temperature on the geopolymerization process of a metakaolin-based geopolymer, Mater. Lett. 65(6) (2011) 995-998. doi:10.1016/j.matlet.2010.12.049

[37]- D. Khale, R. Chaudhary, Mechanism of geopolymerization and factors influencing its development: a review. J. Mater. Sci. 42 (2007) 729-46. doi:10.1007/s10853-006-0401-4

[38]- S. Alonso, A. Palomo, Alkaline activation of metakaolin and calcium hydroxide mixtures: influence of temperature, activator concentration and solids ratio. Mater Lett. 47(1–2) (2001) 55–62. doi:10.1016/S0167-577X(00)00212-3

[39]- A.A. Adam, Strength and Durability Properties of Alkali Activated Slag and Fly Ash-Based Geopolymer Concrete. PhD thesis, Civil, Environmental and Chemical Engineering, RMIT University, 2009.

[40]- V.F.F. Barbosa, K.J.D. Mackenzie, C. Thaumaturgo, Synthesis and Characterisation of Sodium Polysialate Inorganic Polymer Based on Alumina and Silica. In: Proceedings of the 2nd Geopolymer International Conference, Saint Quentin, France, 1999, pp. 65-77.